



World Scientific News

An International Scientific Journal

WSN 112 (2018) 226-234

EISSN 2392-2192

SHORT COMMUNICATION

Higher Solar Cell Efficiency Achieved with ZnO/Si heterojunction

Ayad jumaah kadhim^{1,2}, Muneer H. Jaduaa Alzubaidy^{1,2}, Ahmed N. Abd^{2,*}

¹College of Science, Wasit University, Wasit, Iraq

²Department of Physics, Faculty of Science, University of Al-Mustansiriyah, Baghdad, Iraq

*E-mail address: ahmed_naji_abd@uomustansiriyah.edu.iq

ABSTRACT

In this work, the zinc oxide nanoparticles were prepared chemically and deposited by casting style on glass bases and treated thermally at a temperature of 600 °C. The study focused on Optical and structural properties of thin films. An optical advantages of Zinc Oxide (ZnO) were characterized by using ultraviolet visible Spectroscopy. And the structure by using X-Ray Diffraction and (AFM). The optical advantages of thin films were studied by recording the transmittance spectra of wavelengths range (300-900 nm). The energy gap was calculated using tauc equation and is found (3 eV). I-V properties of the solar cell under light at 40 mW/cm² flounce was investigated. The open circuit Voltage (V_{oc}) was 33 and Short-circuit density (I_{sc}) was 0.017 mA. This measurements show that the fill factor (F.F) and conversation efficiency (η), were 55% and 9.9% respectively.

Keywords: AFM, chemical method, XRD, solar cell, conversation efficiency, ZnO/Si

1. INTRODUCTION

II-VI semiconductor compound, such as ZnO/Si used in many applications in a wide range of devices it is the material transparent conducting oxides (TCO) whose thin films attract

much interest due to its typical properties such as high mechanical and chemical stability and high optical transparency in the visible and near-infrared regions. ZnO it can be used as an anti-reflecting coating layer for solar cells [1]. Many studies have been done on ZnO by using a different film growth techniques as sputtering technique, Thermal vacuum evaporation, spray pyrolysis and chemical deposition techniques. The drop-casting is traditional method for obtained ZnO. Thin Films because it's low cost, simple and low waste production. The structural of Zinc Oxide is a mixture of hexagonal and cubic structure depend on the manufacturing conditions. The electronic transport mechanism in polycrystalline thin films strongly depends on their structure. XRD technique was used to measure the crystalline structure and grain size of the thin films [2]. ZnO is n-type semiconductor, Zinc oxide exhibits a wurtzite or cubic structure. Zinc Oxide is more stability with the hexagonal structure. The lattice constants of bulk zinc oxide around ($a = 0.32495$ nm) and ($c = 0.52069$ nm) at (300 K) with a c/a ratio of 1.602, which is close to the 1.633 ratio of an ideal hexagonal close-packed structure [3,4]. The optical properties of a thin films depend strongly on the magnification technique. Two of most important optical properties are extinction coefficient and refractive index are called the optical constants. In many researches the optical constants were determine by transmittance through a thin film of the material prepared on substrates. That due to electronic transitions between the valance and conduction bands is split into direct and indirect transitions [5].

2. EXPERIMENTAL DETAILS

10.88g of ZnO was dissolved in 80 ml of PVC and ethanol (99.9%). The solution was put into stirring. The Suspended material was saved at 75 °C for 1hour. After cooling the dissolved material at R.T, the particles were separated by centrifugation and were washed with ethanol to remove any wastes.

XRD (6000 shimadzu) was used to studied the crystallize of nanoparticles. The solubility of nanoparticles solution was measured by using (UV-1800, Shimadzu) [11-13].

3. RESULTS AND DISCUSSION

XRD pattern of ZnO thin films prepared by chemical method were shown in Figure 1. Three peaks at $2\theta = 31.62^\circ$ and 34.30° and 36.13° corresponds to (100), (002) and (101) planes were observed respectively, which belong to ZnO (JCPDS card no 036-1451), the crystallite size (D) was measured by using Scherer's formula [6].

$$D = 0.94\lambda/\beta\cos\theta \quad (1)$$

where λ is the X-Ray wavelength (0.15405 nm), θ is the brag's angle and β is the full width at half maximum (FWHM) of the diffraction beak in radians. The dislocation density (δ) and microstrain (γ) values are measured by using the following relation [7].

$$\gamma = 1/D^2 \quad (2)$$

$$\gamma = \beta \cos\theta / 4 \tag{3}$$

The measurements of grain size, microstrain and dislocation values are present in Table 1.

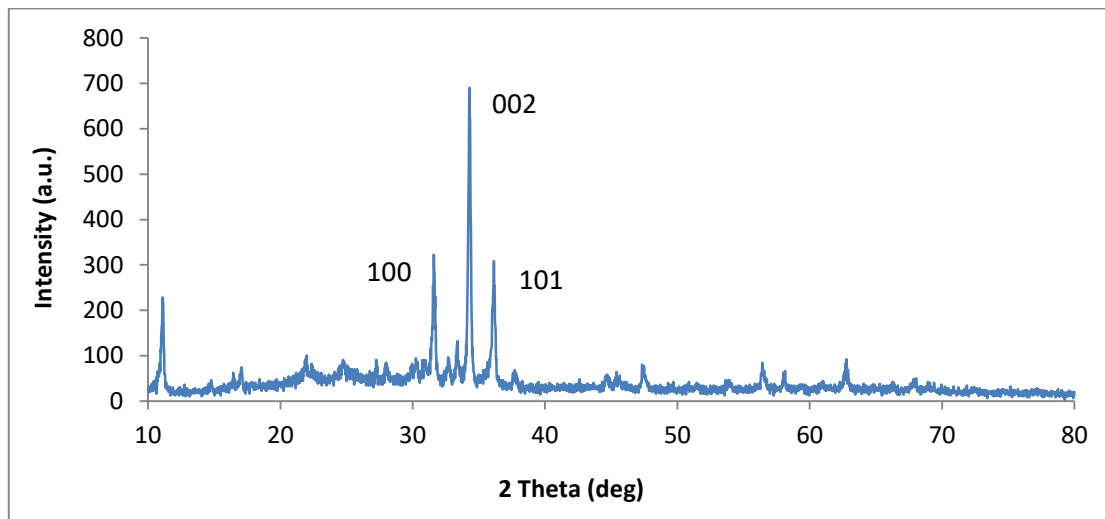


Fig. 1. XRD pattern of ZnO nanoparticles, which obtained by the chemical method is precipitated by drop casting technique on a glass substrate at annealing temperature of 600°C.

Table 1. XRD properties of ZnO nanoparticles at 600 °C.

2θ (deg)	(hkl) planes	B (deg)	D (nm)	$\delta \times 10^{14}$ lines·m ⁻²	$\gamma \times 10^{-4}$ lines ⁻² ·m ⁻²
31.63	100	0.279	45.829	4.76	7.56
34.30	002	0.301	36.694	7.42	9.44
36.13	101	0.417	41.944	5.68	8.26

The microstrain and dislocation density of ZnO nanoparticle films which prepared by chemical reaction were listed in Table 1.

Figure 2 appears 3D AFM picture and Granularity accumulation distribution plot of ZnO thin films fabricated by the chemical method is deposited on the glass Base at (600 °C). AFM image show that the grains are uniformly distributed within the scanning (4000×4000) nm with individual vertical grains extending to the up. ZnO NPS has a hemispherical shape with very good homogeneous granules, homogenously homogeneous. The measured RMS values for surface roughness and average grain size are shown in Table 2.

Figure 3 shows the transmission spectra of ZnO film. The data is corrected for glass transmission in UV region. Also, the figure appear the transmission spectra increase with increasing the wavelength.

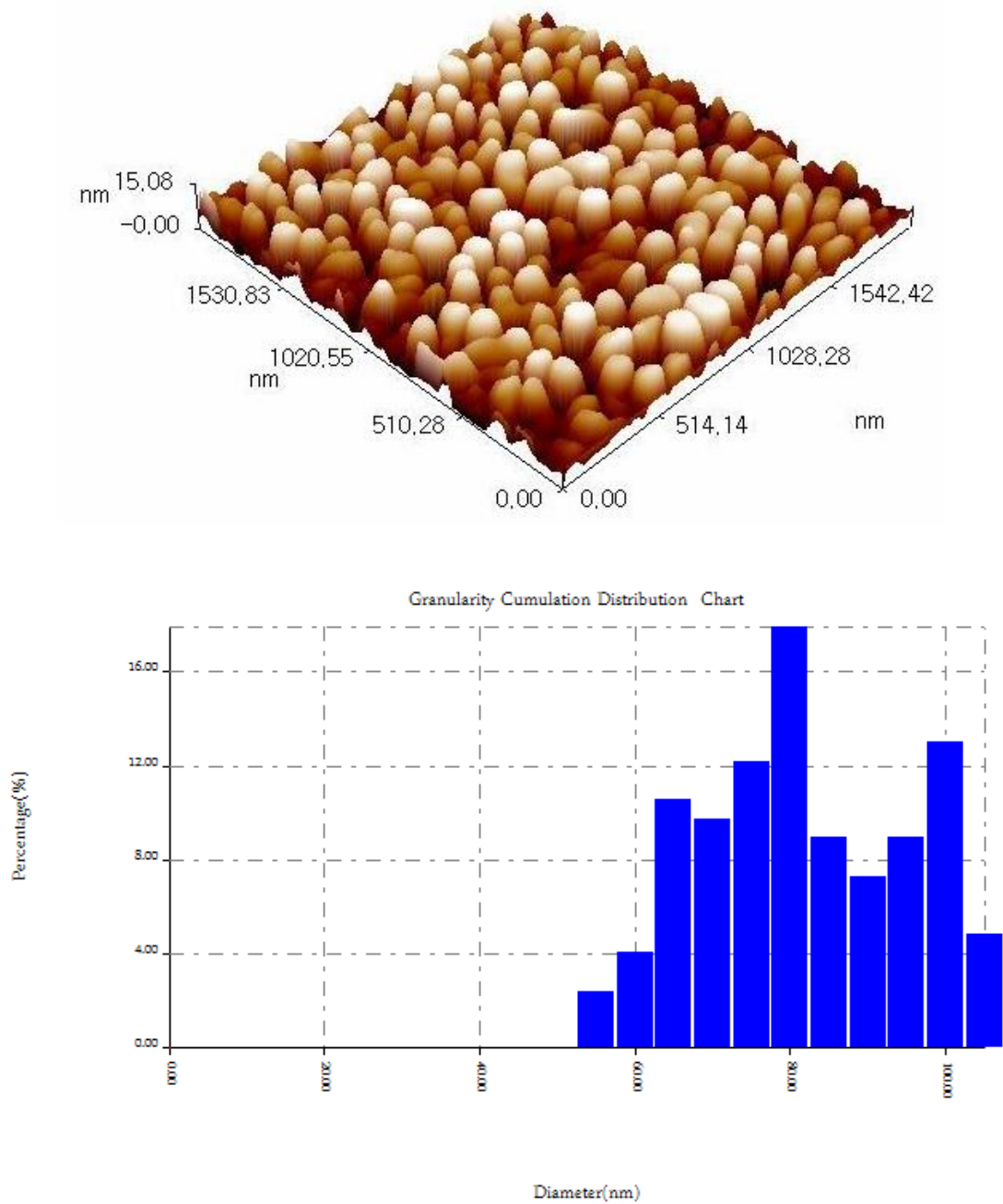


Fig. 2. 3D AFM images of ZnO NPs surface and granularity accumulation distribution chart at temperature annealing 600 °C.

Table 2. Average diameter size, roughness and root mean square of ZnO nanoparticles

Average diameter size (nm)	Roughness density (nm)	RMS (nm)
79.18	3.77	4.35

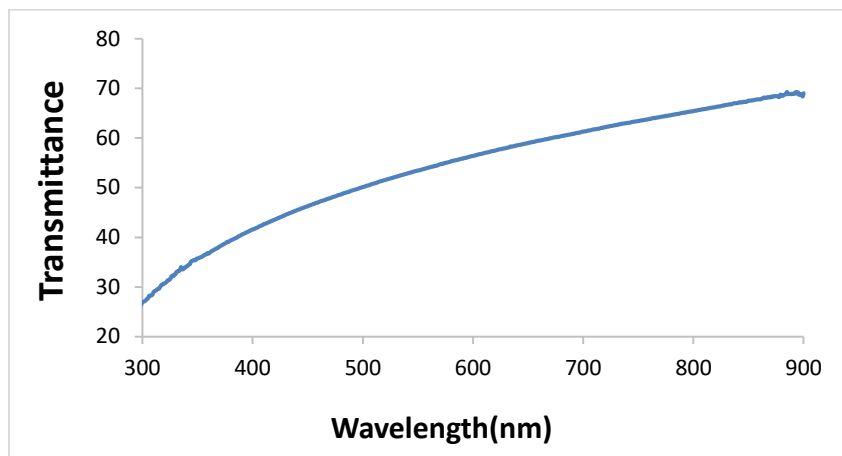


Fig. 3. Transmission spectra of ZnO nanoparticles

Absorption spectrum shows in Fig 4. It was clear that there was a sharp decrease in absorption while reducing the wavelength.

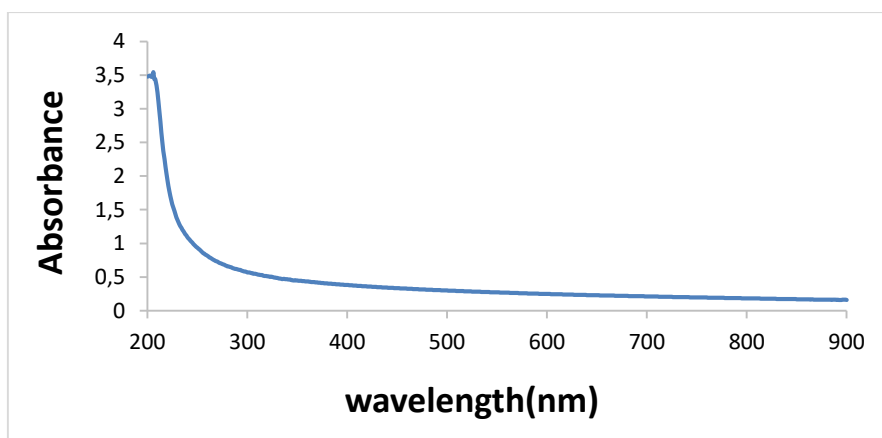


Fig. 4. Absorbance of the ZnO nanoparticles

(T) and (A) are the transmittance and absorbance respectively of the ZnO film. The reflectance of the film has been found by using equation:

$$T+A+R=1 \tag{4}$$

ZnO thin film reflection increases with wavelength increases as shown in Fig. 5 due to increased transmittance.

The α coefficient was measured with $\alpha = 0.30 ((h\nu - E_g)$ when $\alpha = 2.303A / t$ and thickness of the thin layer, $h\nu$ is the energy of the photon, $E_g = 1240 / \lambda$ (nm) and $n = 0.5$ for the allowed direct transmission with it. The graph between $(\alpha h\nu)^2$ versus photon energy ($h\nu$) gives the value of the direct band gap. The estimation of the straight line to $\alpha h\nu^2 = 0$ gives the value of

the band gap, as shown in Fig. 6. The optical band gap is 3 eV. This result is very important to judge whether this film can be used in the solar cell system.

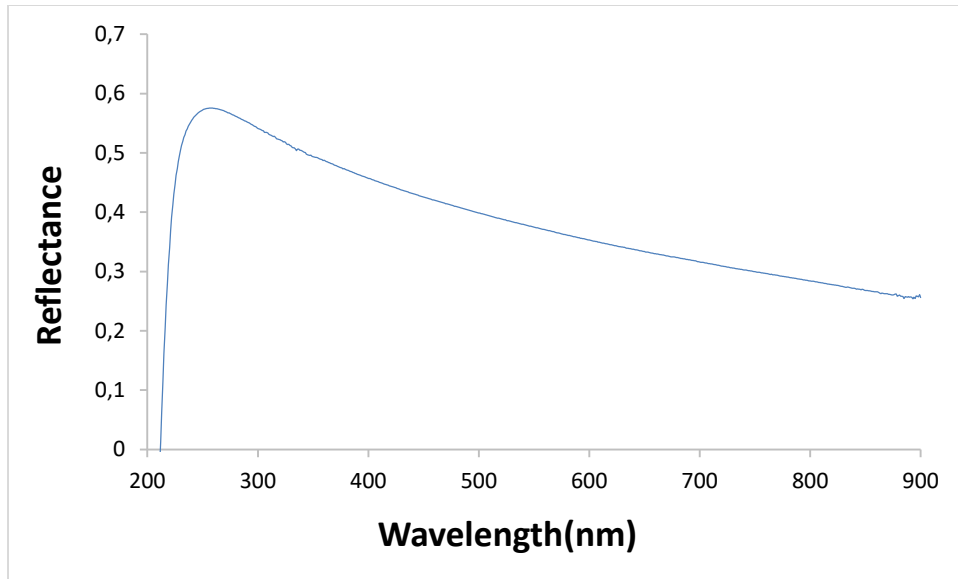


Fig. 5. Reflectance spectrum of ZnO thin film

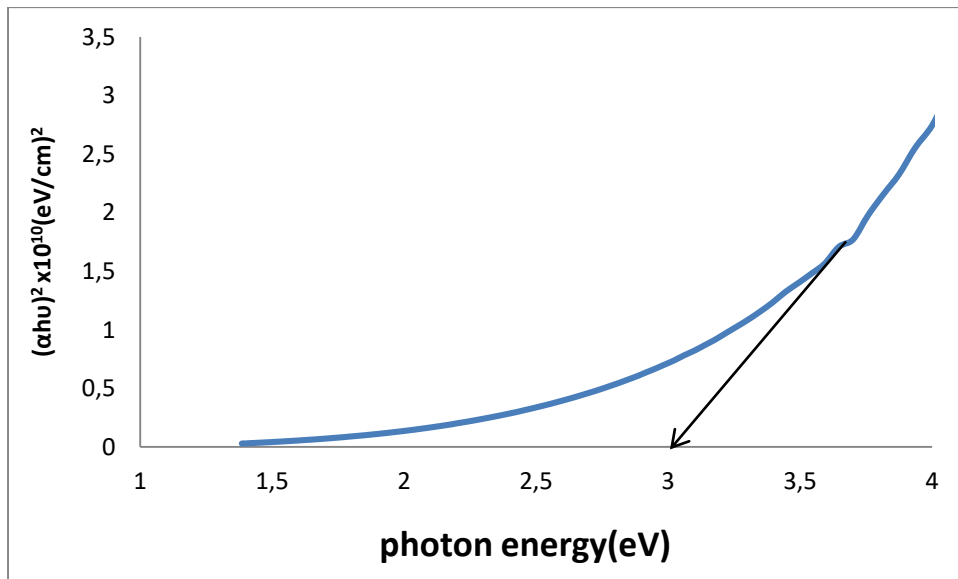


Fig. 6. $(\alpha h\nu)^2$ against photon energy graph of ZnO thin films

Using the reflectance R of the thin film, the refractive index can be measured from the following equation [8]:

$$n = (1 + R^{0.5}) / (1 - R^{0.5}) \quad (5)$$

The refractive index (n) of the prepared ZnO films has been measured using equation 5, for a range of wavelength of (300-900 nm). The graph of n against wavelength was appeared in Figure 7. The refractive index of the film decrease with increasing the wavelength.

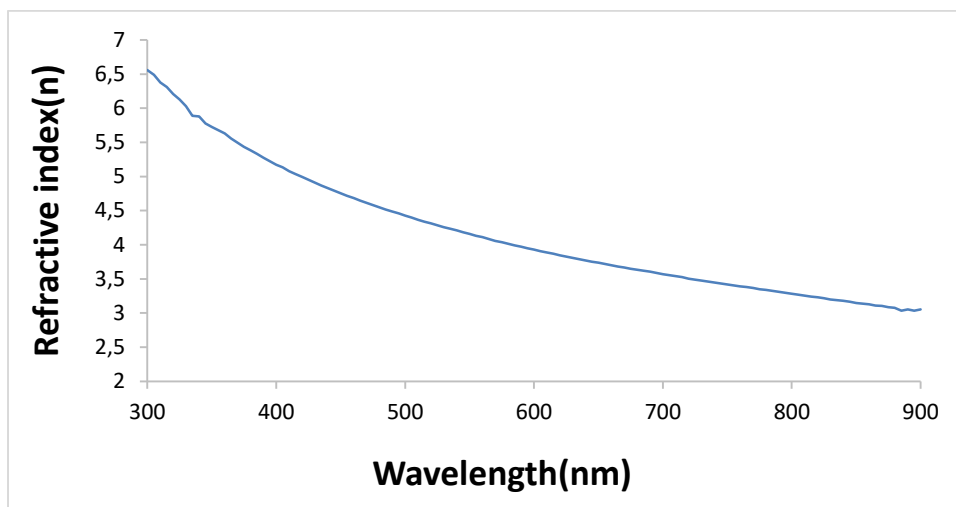


Fig. 7. Refractive index spectrum of ZnO thin films

Fig. 8. appears the I-V dark properties in forward and reverse direction of n-ZnO/P-Si solar cell.

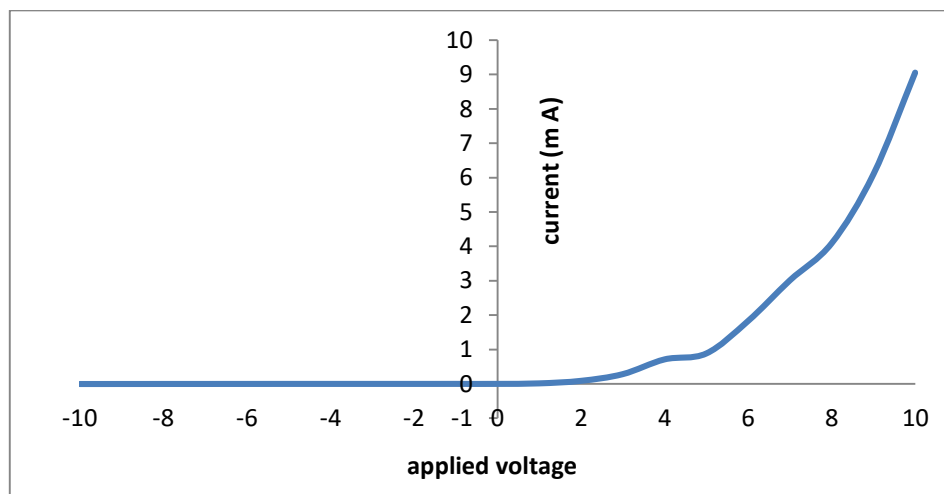


Fig. 8. I-V characteristics under forward and reverse bias of n-ZnO/P-Si at 600 °C.

Figures 8 and 9 show that the properties of the current reflective voltages of the instrument are calculated in the dark and the optical current is less than $40 \mu\text{W} / \text{cm}^2$ of tungsten mass light. It can be observed that the current inverse value of a particular voltage of the solar cell n-ZnO / P-Si under the light is higher than those in the dark and can be seen from these figures that the current value of a given voltage in order for the heterojunction under light is higher in

darkness, That the resulting light created a photocurrent contribution due to the production of electronic holes due to light absorption. This behavior yield useful information on the electron-hole pairs, which are effectively created in the junction by incident photons [9].

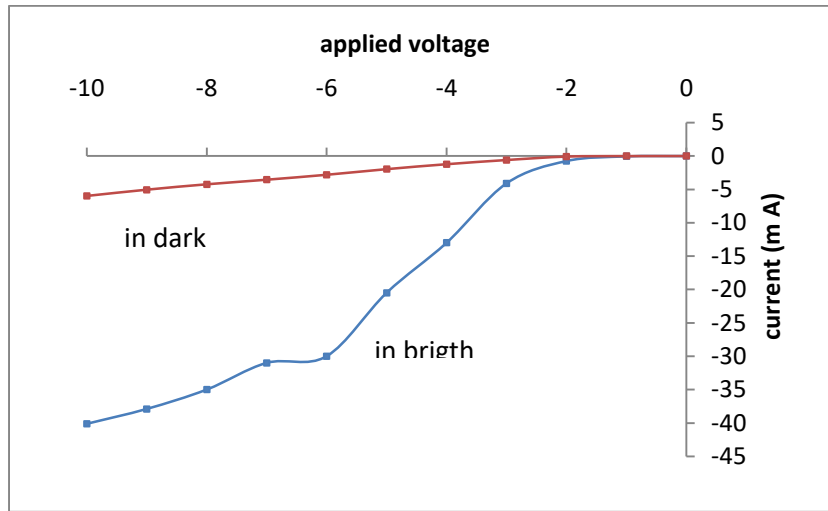


Fig. 9. Illuminated (I-V) characteristics of n-ZnO/P-Si solar cell at 600 °C.

Figure 10 appears the I-V properties of the solar cell under a 40 mW/cm² light condition.

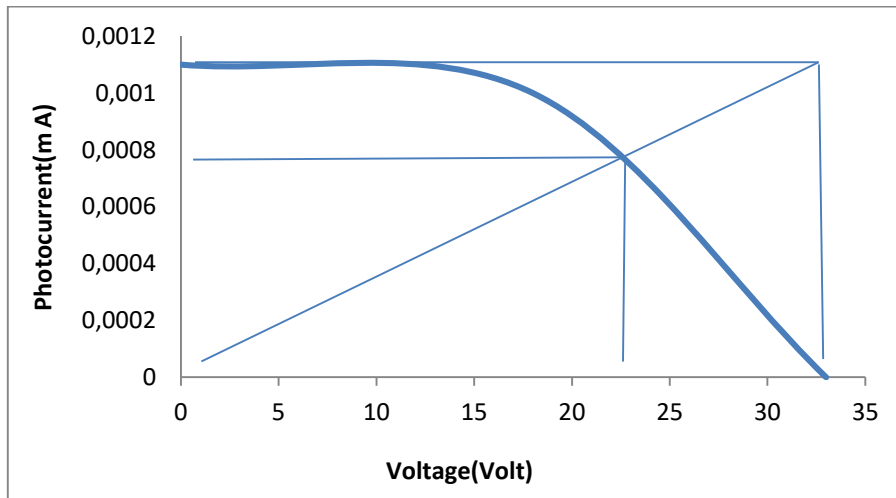


Fig. 10. Characteristics of n-ZnO/P-Si solar cell at 600 °C.

The present study, the n-ZnO/P-Si solar cell has an open circuit voltage (V_{oc}) of 33 V, a short circuit current (I_{sc}) of 0.017Ma, a maximum voltage (V_{max}) of 25V, and a maximum current (I_{max}) Of 0.0125 mA.

The fill factor (F.F) measured as following [10].

$$F.F = (P_{\max} / V_{oc} \times i_{sc}) \times 100\% \quad (6)$$

F.F was measured to be 55%

Cell energy transformation efficiency (η), was measured using relation (7)

$$H = (P_{\max} / P_{in} \times a) \times 100\% \quad (7)$$

where P_{in} is the power input to the cell characterized as the total shining energy incident on the surface of the solar cell in mW/cm^2 , A is the surface area of the solar cell in cm^2 and $P_{\max} = V_{\max} \times I_{\max}$ [10]. The efficiency of the (n-ZnO/P-Si) solar cell was 9.9% using the chemical reaction

4. CONCLUSIONS

ZnO Thin films were successfully prepared in a chemical way. The value of the band gap is 3eV estimated by the optical characterization. X-Ray diffraction patterns (XRD) show that zinc oxide is multicrystalline. The properties of n-ZnO / P-Si show good results to ensure that this device is suitable for applications of solar cells.

References

- [1] H. Kim, C. M. Gilmore, Zinc Oxide bulk, Thin films and Nano structures. *Appl. Phys. Lett.* V. 76, (2000) 259.
- [2] B. Murate, *Turk. J. Phys.* V. 28, (2004) 379.
- [3] R. Baron, F. W. Campbell, I. Streeter, L. Xiao, R. G. Compton, *Int. J. Electrochem. Sci.* V. 3. (2008) 556.
- [4] Todd Stiner, Semiconductor Nanostructures for optoelectronic Applications. Artech House, ISBN 1 (2004). 58053-751-0, Boston-London.
- [5] S. Lindroos and G. Rusu, *J. Optoelectron. Adv. Materials*, V. 7, No. 2, (2005) 817.
- [6] E. Kashevsky, V.E. Agabekov, S.B. Kashevsky, K.A. Kekalo, E.Y. Manina, I.V. Prokhorov, V.S. Ulshchikk, study of cobalt ferrite nanosuspensions for low-frequency ferromagnetic hyperthermia. *Particology* 6 (2008) 322-333.
- [7] W.L. Bragg, The Structure of Magnetic and the spinels, *Nature* 95 (1915) 561-561.
- [8] B.D. Cullity, Element of X-ray diffraction, Addison-Wesley, Reading, (1972) 102.
- [9] S.A. Taha, I.M. Ibrahim, N.A. Khalefa, I-V Characteristic of CdO/PS Heterojunction, *IJAIEEM* 3 (2014) 143-148.
- [10] N.E. Makori, I.A. Karimi, and W.K. Njoroge, characterization of SnSe-CdO: Sn Pn junction for solar cell applications, *International Journal of Energy Engineering* 5 (2015) 1-4.
- [11] Z.W Pan, *et al. Science*, 291 (2001), p. 1947
- [12] M.S Arnold, *et al. J. Phys. Chem. B*, 107 (3) (2003), p. 659
- [13] E Comini, *et al. Appl. Phys. Lett.* 81 (10) (2002), p. 1869